Journal of Dispersion Science and Technology
Publication details, including instructions for authors and subscription information:
http://www.tandfonline.com/loi/ldis20

Effect of Surfactants on the Formation, Morphology, and Surface Property of Synthesized SiO_2 Nanoparticles

Wei Wang [a], Baohua Gu [a] & Liyuan Liang [a b]
[a] Environmental Sciences Division, Oak Ridge National Laboratory, P.O. Box 2008, Oak Ridge, Tennessee, 37831, USA
[b] School of Engineering, Cardiff University, Cardiff, UK
Version of record first published: 17 Mar 2008.

To cite this article: Wei Wang , Baohua Gu & Liyuan Liang (2005): Effect of Surfactants on the Formation, Morphology, and Surface Property of Synthesized SiO_2 Nanoparticles, Journal of Dispersion Science and Technology, 25:5, 593-601

To link to this article: http://dx.doi.org/10.1081/DIS-200027309

JOURNAL OF DISPERSION SCIENCE AND TECHNOLOGY
Vol. 25, No. 5, pp. 593–601, 2004

Effect of Surfactants on the Formation, Morphology, and Surface Property of Synthesized SiO_2 Nanoparticles

Wei Wang,[1,*] Baohua Gu,[1] and Liyuan Liang[1,2]

[1]Environmental Sciences Division, Oak Ridge National Laboratory, Oak Ridge, Tennessee, USA
[2]School of Engineering, Cardiff University, Cardiff, UK

ABSTRACT

This study investigated the effect of cationic, anionic (saturated and unsaturated), and nonionic surfactants on the formation, morphology, and surface properties of silica nanoparticles synthesized by the ammonium-catalyzed hydrolysis of tetraethoxysilane in alcoholic media. Results indicate that at a relatively low surfactant concentration (1×10^{-3}–1×10^{-6} M), cationic surfactants significantly affected the growth of silica particles as measured by dynamic light scattering and transmission electron microscopic analyses. In contrast, the anionic and nonionic surfactants showed relatively minor effects in the low concentration range. The magnitude of negative zeta potential was reduced for silica colloids that were synthesized in the presence of cationic surfactant because of charge neutralization. The presence of anionic surfactants only slightly increased the negative zeta potential while the nonionic surfactant showed no obvious effects. At high surfactant concentrations ($>1 \times 10^{-3}$ M), cationic and anionic surfactants both induced colloid aggregation, while the nonionic surfactant showed no effect on particle size. Raman spectroscopic analysis suggests that molecules of cationic surfactants adsorb on silica surfaces via head groups, aided by favorable electrostatic attraction, while molecules of anionic and nonionic surfactants adsorb via their hydrophobic tails.

Key Words: Silica; Surfactant; Nanoparticle; Colloid; Raman spectra; Synthesis.

INTRODUCTION

The preparation of monodispersed colloidal particles by controlled hydrolysis of metal alkoxides has been widely investigated for a number of inorganic materials. In particular, silica (SiO_2) colloids have received considerable attention in the literature since Stöber et al.[1] showed that hydrolysis of silicon alkoxides

*Correspondence: Wei Wang, Environmental Sciences Division, Oak Ridge National Laboratory, P.O. Box 2008, Oak Ridge, TN 37831, USA; E-mail: wangw@ornl.gov.

DOI: 10.1081/DIS-200027309
0193-2691 (Print); 1532-2351 (Online)

leads to the precipitation of essentially spherical SiO_2 colloidal particles. In general, particle formation involves complex processes, including nucleation, particle growth, and dissolution. For SiO_2 colloids, a large number of experimental investigations have focused on particle morphology, size control, and growth mechanism.[2] These studies revealed that the diameter and the size distribution of SiO_2 spheres strongly depend on the reaction conditions, including tetraethoxysilane (TEOS)/H_2O/NH_3 concentration ratios, solvent type, and temperature.[3–9] Self-assembled surfactant templates, such as micelle and microemulsion, also have been widely used to control particle morphology in SiO_2 synthesis.[10,11] However, little work has been done on the effect of adsorbed surfactants at low concentrations on particle morphology during synthesis. Surfactants in the preparation media could influence nucleation, particle growth, and particle interactions, which has been largely overlooked to date.[12] This research was therefore aimed at investigating the effect of different types of surfactants—including cationic, anionic, and nonionic surfactants—on the formation, particle sizes, polydispersity, and surface properties of SiO_2 colloids.

EXPERIMENTAL

Materials

TEOS ($\geq$99%), cetyltrimethylammonium bromide (CTAB, $\geq$99%), sodium dodecyl sulfate (SDS, $\geq$99%), and sodium oleate (NaOl, $\geq$99%) were purchased from Fluka. Brij®30 [polyoxyethylene(4) dodecyl ether, $C_{12}E_4$] was an Aldrich product. Absolute ethanol (AR) was obtained from EM Scientific, and $NH_3 \cdot H_2O$ (29.5%) came from J. T. Baker. All chemicals were used as received. Deionized water with a resistivity of 18.2 MΩ cm was obtained from a Millipore ultra-pure water system.

Colloid Synthesis

Monodispersed colloidal SiO_2 spheres were prepared by hydrolysis of TEOS in ethanol medium in the presence of water and ammonia using a modified procedure that was originally described by Stöber et al.[1] Hydrolysis and condensation of the TEOS monomers catalyzed by ammonia produce spherical SiO_2 particles, which exhibit a negative, stabilizing surface charge in water due to the ionization of the surface hydroxyl functional groups.[13] A typical preparation is to rapidly mix two equal-volume reagent solutions under vigorous stirring conditions. One solution contains ethanol and TEOS, while the other includes ethanol, water, ammonia, and surfactant; the two yield a total volume of 250 mL. To study the effect of surfactants on the formation and surface properties of SiO_2 colloids, we fixed the concentrations of TEOS (0.2 M), NH_3 (0.12 M), and H_2O (9.0 M) but varied the concentrations and the types of surfactants in the synthesis. The reaction mixture usually began to turn a turbid white in about 5–15 min as SiO_2 particles were formed. The reaction was allowed to continue for $\sim$12 hr for completion at room temperature.

Measurements

The particle size and the size distribution of SiO_2 colloids were determined by dynamic light scattering (DLS); their zeta (ζ) potentials were determined by electrophoretic light scattering (ELS) using a Brookhaven 90Plus/ZetaPlus instrument. For size measurements, samples were prepared by mixing an aliquot of 0.2 mL of SiO_2 colloids with 2.0 mL of 1 mM NaCl solution in a cuvette, while samples were directly transferred into the cuvette for ζ potential measurements. All measurements were performed at a scattering angle of 90° for signal collection.

Direct imaging of colloidal particles was obtained by a Hitachi F 4000 transmission electron microscope (TEM) under an acceleration voltage of 200 kV. A drop of colloidal suspension was placed on a formvar/carbon film supported by a 300 mesh copper grid (Ted Pella Ltd.), and the solvent was allowed to evaporate to dryness before analysis.

Raman spectra of the surfactants sorbed onto SiO_2 particles were recorded using a Renishaw Raman spectrometer equipped with a Leico microscope and a 785-nm laser. The spectral resolution was 2–3 cm^{-1}. The wet SiO_2 nanoparticles collected by centrifuge were placed on quartz slides and allowed to dry before measurements. The spectra were normalized with the intensity of the Si—O vibrational band at 486 cm^{-1}. Control experiments were also performed using the pure SiO_2 colloids (without surfactants) or the same background surfactant solution (1×10^{-3} M) sorbed onto a quartz plate surface.

RESULTS AND DISCUSSION

Synthesis of silica nanoparticles using a recipe of 0.2 M TEOS/9.0 M H_2O/0.12 M NH_3 in ethanol usually produces negatively charged, monodisperse

spherical particles with diameters of ~108 nm and a polydispersity of ~5–10%.[14] Depending on the type and the concentration of surfactants, the surfactant additives affected the rate of particle formation and growth in the hydrolysis reaction. In absence of surfactants, in situ DLS measurements showed that the light scattering due to the formation of colloidal particles reached maximum intensity after ~70 min of hydrolysis reaction of TEOS. The presence of the cationic surfactant, CTAB and the anionic surfactants, SDS and NaOl showed an accelerated effect on colloidal particle formation, while the presence of the nonionic surfactant, $C_{12}E_4$ had little effect on formation rate. For example, at a surfactant concentration of 1×10^{-3} M, the light scattering intensity of the colloidal suspension reached its maximum when the hydrolysis reaction had proceeded for 50 min for CTAB, ~20 min for SDS and NaOl, and ~68 min for $C_{12}E_4$. All reactions appeared to have reached equilibrium (no changes in particle size) after ~300 min as measured by the DLS.

The effect of surfactants on the size of synthesized SiO_2 particles depended on surfactant type and concentration (Fig. 1). The addition of the cationic surfactant CTAB reduced the average size of SiO_2 colloid particle from ~108 to ~75 nm with an increase in the CTAB concentration up to 3×10^{-4} M. With a similar concentration the anionic surfactants SDS and NaOl did not show significant effects on the particle size. Both the cationic and anionic surfactants had little effect on SiO_2 colloidal polydispersity (~5–10%) at the low concentrations. However, at a surfactant concentration of $\sim 1 \times 10^{-3}$ M, the presence of either cationic or anionic surfactant substantially increased the particle size and polydispersity (~10–20%) of SiO_2 colloids. With further increases in surfactant concentrations, SiO_2 particle size dramatically increased to larger than 500 nm and polydispersity increased to ~20–40%, suggesting that both cationic and anionic surfactant molecules induced aggregation of primary particles of SiO_2 colloids. The nonionic surfactant, $C_{12}E_4$ showed little effect on the size or size distributions of synthesized SiO_2 colloidal particles for the entire surfactant concentration range studied.

The presence of surfactants during synthesis also affected the surface charge properties of the resulting SiO_2 colloids as a result of interaction of surfactants with the charged SiO_2 surfaces (Fig. 2). In the absence of surfactant, the ζ potential of SiO_2 colloids is about −54 mV. With the addition of surfactants, cationic CTAB gradually reduced the negative ζ potential of SiO_2 particles as a result of surface charge neutralization by positively charged CTA^+ ions. In contrast, the anionic SDS and NaOl gradually increased the magnitude of the negative ζ potential, while the nonionic $C_{12}E_4$ showed little effect on surface potential changes of SiO_2 particles and was nearly independent on the $C_{12}E_4$ concentration.

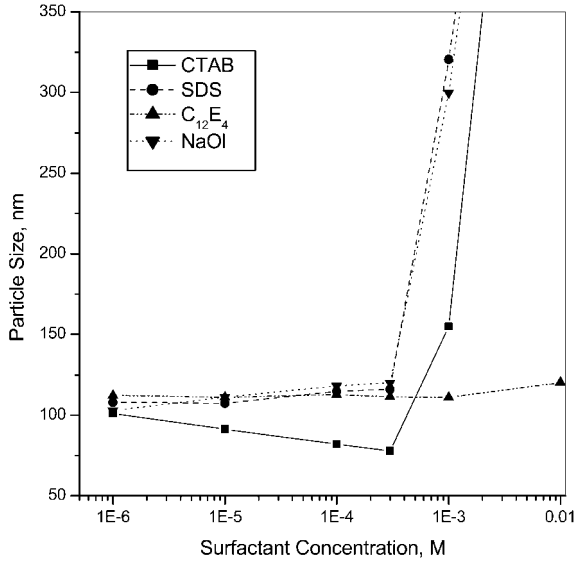

Figure 1. Effects of surfactant additions on the growth and size distributions of synthesized SiO_2 nanoparticles. A recipe of [TEOS] = 0.2 M, $[NH_3]$ = 0.12 M, $[H_2O]$ = 9.0 M in ethanol was used for the synthesis. In the absence of surfactants, the average particle size is ~108 nm with a polydispersity of ~5–10%.

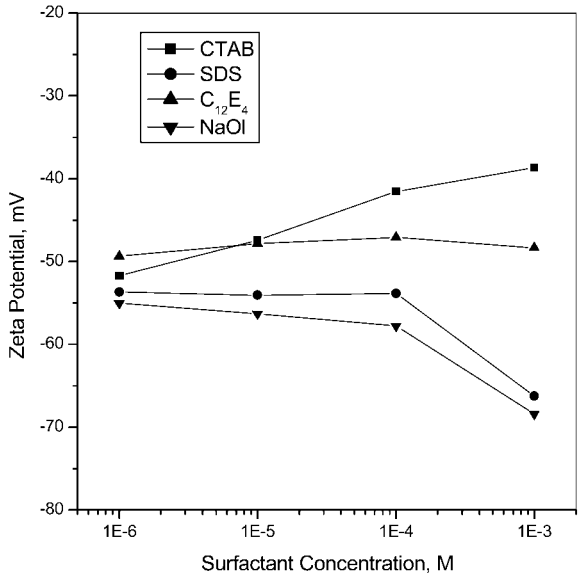

Figure 2. Zeta potentials of synthesized SiO_2 colloids as a function of different surfactants at various concentrations. Without surfactants, the ζ potential is approximately −54 mV.

Cationic Surfactant

The effect of the cationic surfactant CATB on the surface morphology of synthesized SiO_2 particles is further illustrated by the TEM images in Fig. 3. At CTAB concentrations below 1×10^{-3} M, spherical colloidal particles were formed, but the particle size decreased with an increase in CTAB concentration [Fig. 3(a) and (b)]. At a CTAB concentration of 1×10^{-3}, silica particles exhibited an uneven surface morphology, with an average size of ~155 nm [Fig. 3(c)]. However, when CTAB concentrations exceeded 3×10^{-3} M, larger particles (~700 nm) were observed in addition to small particles (~200 nm) [Fig. 3(d)]. The aggregation of silica particles at a relatively high CTAB concentration could be partially attributed to interactions between negatively charged SiO_2 particles and positively charged CTA^+ ions, but no effects from surfactant micelles were observed. The critical micelle concentration (CMC) of CTAB is $\sim 9.0 \times 10^{-4}$ M in water,[15] while it is much higher in alcoholic media.[16] No micelles formed within the surfactant concentration range studied in this work.

The experimental observations suggest that the effect of cationic surfactant, CTAB, on synthesis of SiO_2 particles is in the stage of SiO_2 growth through sorptive interaction via favorable electrostatic pathways. Sorption of the cationic surfactant CTAB on silica quartz surfaces has been widely studied, although direct spectroscopic evidence of CTAB sorption on colloidal SiO_2 has yet to be documented.[17–19] We examined SiO_2 nanoparticles synthesized in the presence and absence of surfactants by Raman spectroscopy. Raman scattering analysis is known to be sensitive and able to provide direct evidence of molecular conformation or interactions of sorbed surfactants.[20–23] For SiO_2 colloids prepared in the presence of CTAB (1×10^{-2} and 5×10^{-4} M), we observed CTAB vibrational bands including CH_2 stretching modes in 3000–2800 cm^{-1} region, the CH_2 scissoring mode at 1449 cm^{-1}, the CH_2 twisting mode at 1302 cm^{-1}, and the symmetric $H_2C–N^+–(CH_3)_3$ mode at 759 cm^{-1} (Fig. 4). These observations clearly indicate the sorption of CATB on SiO_2 colloidal surfaces in comparison with the vibrational modes of pure CTAB[24,25] and those of pure SiO_2 colloid. In particular, at low CTAB concentrations ($<1 \times 10^{-3}$ M), the CH_2 asymmetric and symmetric

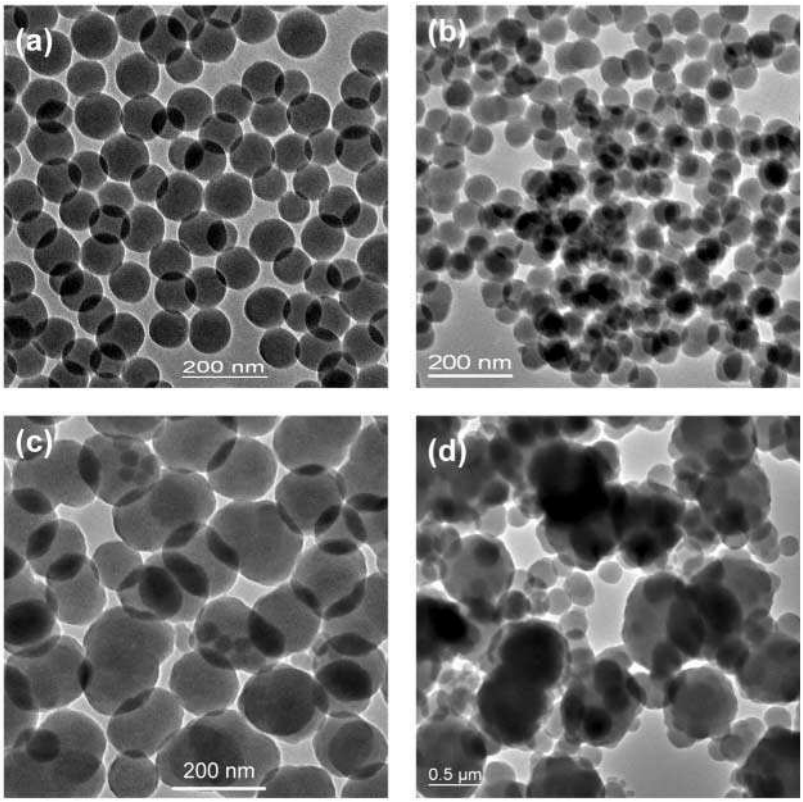

Figure 3. TEM images of SiO_2 spheres synthesized at CTAB concentrations of (a) 3×10^{-6} M, (b) 3×10^{-4} M, (c) 1×10^{-3} M, and (d) 3×10^{-3} M.

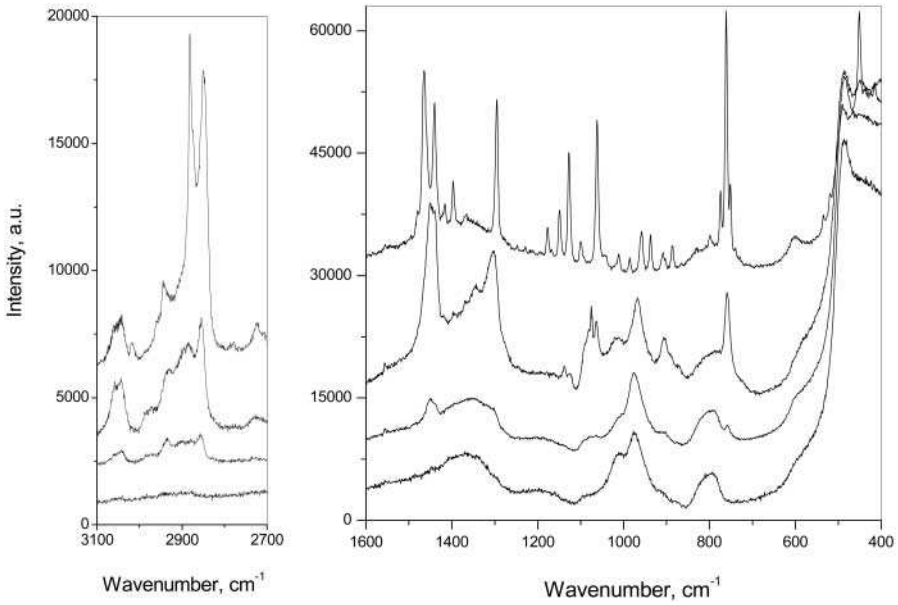

Figure 4. Raman spectra of pure CTAB (a) (from top to bottom), SiO_2 nanoparticles synthesized at the CTAB concentrations of 1×10^{-2} M (b) and 5×10^{-4} M (c), and pure SiO_2 nanoparticles (d).

stretching appeared at 2886 and 2857 cm^{-1}, blue-shifted 5 and 7 cm^{-1} relative to those of pure CTAB, indicating a liquid-like state of CTAB molecules sorbed on SiO_2 surfaces. At higher CTAB concentrations ($\geq 1 \times 10^{-3}$ M), the intensity of CTAB vibrational bands increased, and CH_2 stretching bands appeared at 2885 and 2854 cm^{-1} respectively, suggesting an increased amount of CTAB adsorption and a more condensed layer of sorbed CTAB on SiO_2 surfaces. For the SiO_2 colloids synthesized at a low CTAB concentration ($< 1 \times 10^{-3}$ M), no Raman signals could be detected after colloidal particles were washed with water,

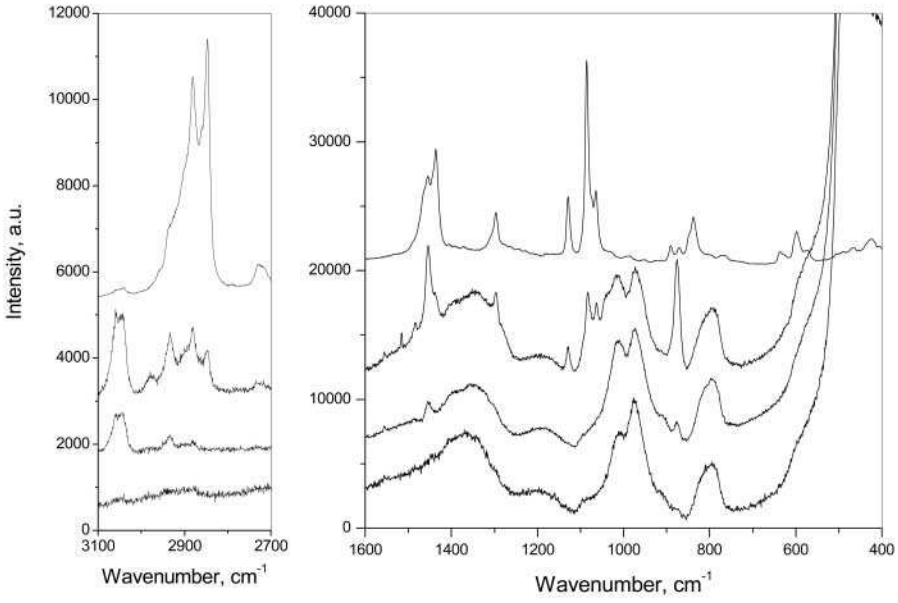

Figure 5. Raman spectra of pure SDS (a) (from top to bottom), SiO_2 nanoparticles synthesized at the SDS concentrations of 1×10^{-2} M (b) and 1×10^{-3} M (c), and pure SiO_2 nanoparticles (d).

indicating no chemical bonding between CTAB and SiO_2. At low concentrations, the adsorbed CTAB layer may have prevented SiO_2 particles from further growth, thus accounting for the smaller particles observed. However, for the SiO_2 colloids synthesized at a higher CTAB concentration ($\geq 1 \times 10^{-3}$ M), not only was there a significant increase in particle size and polydispersity but Raman signals of CTAB also remained after the colloid was washed with water. This implies that some CTAB molecules were entrapped in the aggregated SiO_2 particles. At high CTAB concentrations, the magnitude of ζ potential was reduced, the charge remained negative i.e., no surface charge reversal occurred, on SiO_2 colloids. This suggests a relatively low CTA^+ coverage on SiO_2 surfaces which could not completely balance the negative charges on the surface. The aggregation of primary SiO_2 particles to form large particles was a result of the partial neutralization of the surface charge as well as of hydrophobic interactions between the aliphatic tail layers of adsorbed CTAB molecules on SiO_2 surfaces.

Anionic Surfactant

In contrast to our findings for the sorption of the cationic surfactant, we observed no Raman signals for sorbed anionic SDS and NaOl surfactants on SiO_2 particles at concentrations below 1×10^{-3} M. These observations were expected because of an unfavorable electrostatic interaction and a weak hydrophobic interaction between negatively charged silica particles and the surfactant molecules. The lack of these anioic surfactants on SiO_2 particles is consistent with the lack of effect on particle size, size distribution, and surface morphology of synthesized SiO_2 particles. With increased surfactant concentration to 1×10^{-3} M, we did observe weak signals with a few distinguished Raman bands at 2934, 2881, 1454, and 876 cm^{-1} for sorbed SDS (Fig. 5), and at 2933, 2884, and 1454 cm^{-1} for sorbed NaOl (Fig. 6). The presence of the anionic surfactants on SiO_2 particles correlated to the observed aggregation behavior as shown by particle size measurements in Fig. 1 at SDS and NaOl concentrations $>1 \times 10^{-3}$ M.

In the spectrum of sorbed SDS (1×10^{-2} M), the bands at 1064 cm^{-1} (SO_3 stretching + trans C–C symmetric stretching) and 1083 cm^{-1} (SO_3 stretching + gauche C–C stretching)[26,27] are similar to those of reagent SDS,[28,29] suggesting an insignificant perturbation of head group symmetry following the adsorption of SDS. If adsorption of SDS occurred via the sulfate group, a significant sulfate group symmetry change would appear, and Raman band shifts would be expected. Instead, we observed an enhanced intensity of the CH_3 stretching band at 2934 cm^{-1} and the CH_3 rocking band at 876 cm^{-1}; these observations suggested inter-

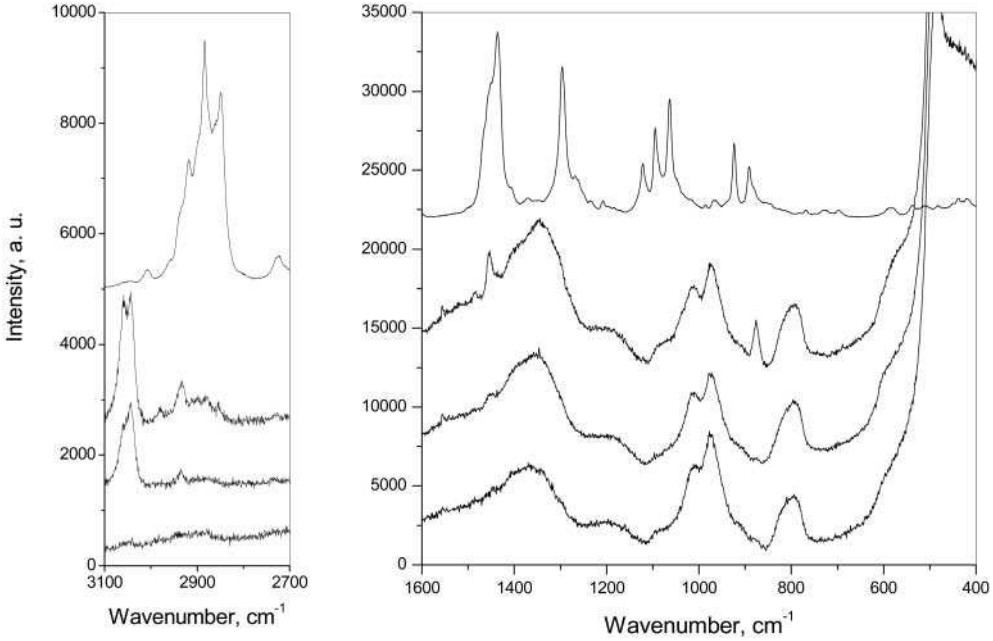

Figure 6. Raman spectra of pure NaOl (a) (from top to bottom), SiO_2 nanoparticles synthesized at the NaOl concentrations of 1×10^{-2} M (b) and 1×10^{-3} M (c), and pure SiO_2 nanoparticles (d).

actions between the terminal CH_3 groups and the SiO_2. In comparison with vibrational bands of pure SDS, the relative intensity of the asymmetric CH_2 stretching band at $2882\,cm^{-1}$ relative to the symmetric CH_2 stretching band at $2848\,cm^{-1}$ increased, indicating a more rigid conformation of the hydrocarbon chains in the adsorbed state. These observations suggest that anionic surfactants may adsorb on SiO_2 colloid surfaces via hydrophobic interaction between surfactant hydrocarbon chains and SiO_2 surfaces.

For SiO_2 colloids synthesized in the presence of 1×10^{-2} M NaOl, the asymmetric stretch of —CH═ red-shifted to $2980\,cm^{-1}$ from $3011\,cm^{-1}$ of pure NaOl and the C═C stretching band at $1656\,cm^{-1}$ disappeared.[30,31] Additionally, the $2933\,cm^{-1}$ band (CH_3 stretch + Fermi resonance) increased in relative intensity, and the band at $875\,cm^{-1}$ (CH_3 rock + C–C stretch) red-shifted $16\,cm^{-1}$ in comparison with that of the pure compound. There is no evidence for structural changes in head groups of sorbed NaOl. The spectroscopic evidence demonstrates that NaOl molecules adsorb on SiO_2 via their C═C double bonds and hydrocarbon chains, as observed for their sorption onto negatively charged metallic colloid surfaces.[32,33]

The hydrophobic interactions are weaker than the electrostatic interactions between surfactant molecules and SiO_2 particles. For example, Roman signals remained when large amount of CTAB was sorbed on SiO_2, whereas Raman signals disappeared after washing SiO_2 colloids sorbed with anionic SDS and NaOl with deionized water. At low surfactant concentrations ($<1 \times 10^{-3}$ M), the anionic surfactants only adsorb on the surface of SiO_2 colloids and do not affect the size of SiO_2 particles during the synthesis (Fig. 1). However, the adsorbed anionic surfactants slightly increased the magnitude of negative ζ potential and thus the stability of SiO_2 colloids (Fig. 2). At a higher surfactant concentration ($\sim 1 \times 10^{-3}$ M) or with an increase of the surface coverage, the adsorption of hydrocarbon chains could have provided a more hydrophobic microenvironment near SiO_2 surfaces to attract more TEOS to hydrolyze and condense, thus producing larger particles ($\sim$300 nm) (Fig. 7). At even higher surfactant concentrations ($>1 \times 10^{-3}$ M), a local head-to-head surfactant bilayer may have formed on the SiO_2 particle surface, leading to an increased surface hydrophobicity and the aggregation of SiO_2 colloids.

Nonionic Surfactant

The presence of the nonionic surfactant $C_{12}E_4$ had no obvious effects on the synthesis of SiO_2 colloids. It only slightly reduced the surface charge density of SiO_2, as shown by the ζ potential measurement (Fig. 2). Raman spectroscopic analysis did not show the sorption of $C_{12}E_4$ at concentrations below 1×10^{-3} M. At a higher concentration ($\geq 1 \times 10^{-3}$ M), we observed C–H stretching bands in the $3000–2800\,cm^{-1}$ region, CH_2 rocking band at $1453\,cm^{-1}$, and CH_3 rocking band at $876\,cm^{-1}$ (Fig. 8). Asymmetric and symmetric CH_2 stretching bands appeared at 2873 and $2852\,cm^{-1}$ for pure $C_{12}E_4$ but were shifted to $\sim$2881 and $2857\,cm^{-1}$ for sorbed $C_{12}E_4$. The spectroscopic observation indicates that the adsorbed surfactant molecules have more flexible conformations, suggesting a weak

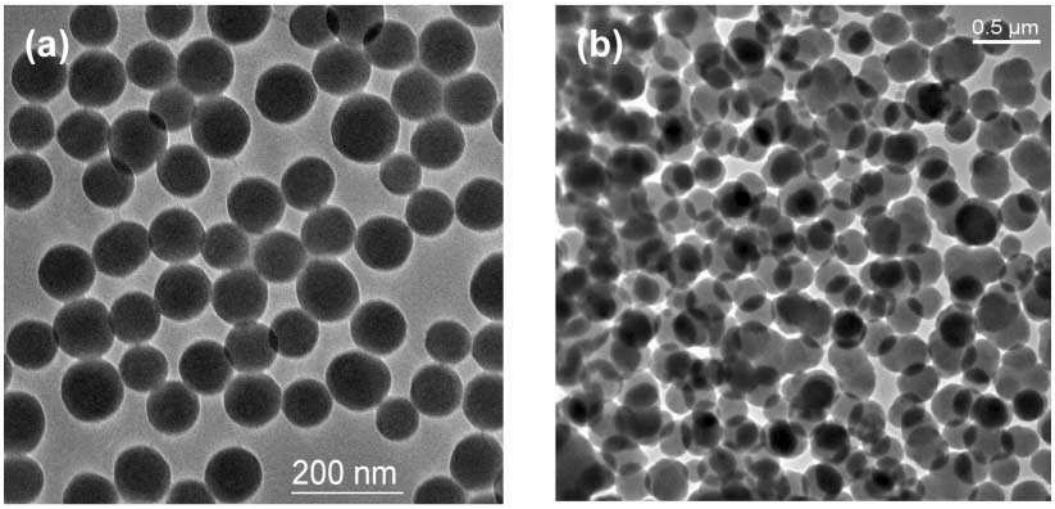

Figure 7. TEM images of SiO_2 spheres synthesized at SDS concentrations of (a) 1×10^{-5} M and (b) 1×10^{-3} M.

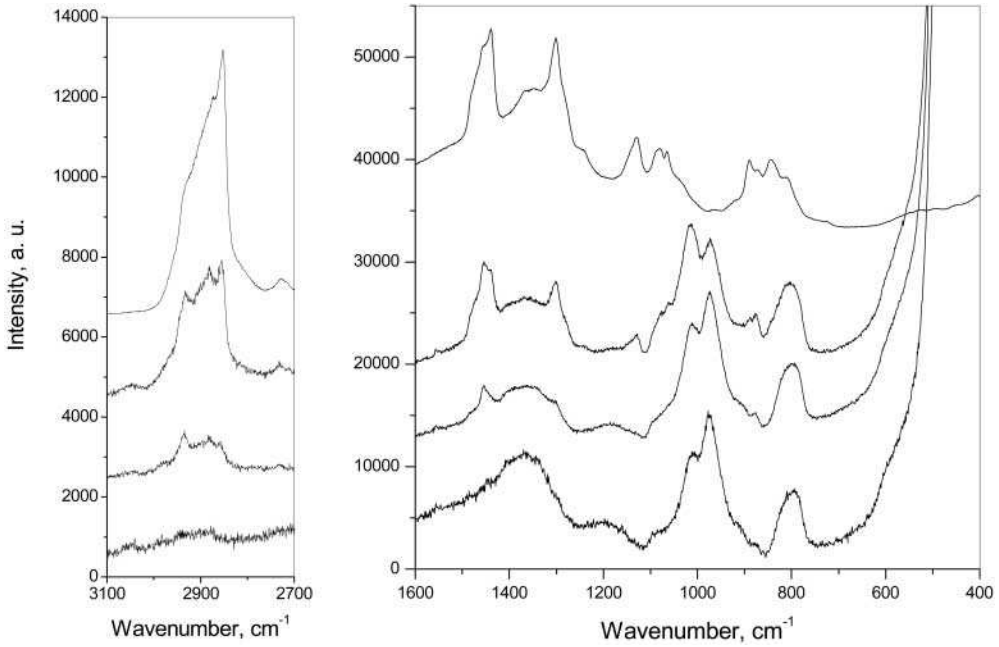

Figure 8. Raman spectra of pure $C_{12}E_4$ (a) (from top to bottom), SiO_2 nanoparticles synthesized at the $C_{12}E_4$ concentrations of 1×10^{-2} M (b) and 1×10^{-3} M (c), and pure SiO_2 nanoparticles (d).

hydrophobic interaction between nonionic surfactants and SiO_2 nanoparticles. As a result, the sorbed surfactants could be readily desorbed by washing the colloid with deionized water. The large volume of the nonionic surfactant molecule and weak interactions between the surfactant and the SiO_2 surface may prevent the aggregation of SiO_2 particles. Therefore, the presence of the nonionic surfactant exhibited little effect on the growth and morphology of SiO_2 particles during the synthesis, even at a high concentration ($\sim 1 \times 10^{-2}$ M).

ACKNOWLEDGMENTS

This research was supported by the Office of Basic Energy Sciences, US Department of Energy, under contract DE-AC05-00OR22725 with Oak Ridge National Laboratory, which is managed by UT-Battelle, LLC.

REFERENCES

1. Stöber, W.; Fink, A.; Bohn, E. Controlled growth of monodisperse silica spheres in micron size range. J. Colloid Interf. Sci. **1968**, *26*, 62–69.
2. Matijević, E. Uniform inorganic colloid dispersions—achievements and challenges. Langmuir **1994**, *10*, 8–16.
3. Bogush, G.H.; Tracy, M.A.; Zukoski, C.F., IV. Preparation of monodisperse silica particles-control of size and mass fraction. J. Non-Cryst. Solids **1988**, *104*, 95–106.
4. Bogush, G.H.; Zukoski, C.F. Studies of the kinetics of the precipitation of uniform silica particles through the hydrolysis and condensation of silicon alkoxides. J. Colloid Interf. Sci. **1991**, *142*, 1–18.
5. Tan, C.G.; Bowen, B.D.; Epstein, N. Production of monodisperse colloidal silica spheres-effect of temperature. J. Colloid Interf. Sci. **1987**, *118*, 290–293.
6. Van Blaaderen, A.; Van Geest, J.; Vrij, A. Monodisperse colloidal silica spheres from tetraalkoxysilanes-particle formation and growth-mechanism. J. Colloid Interf. Sci. **1992**, *154*, 481–501.
7. Zerda, T.W.; Hoang, G. Effect of solvents on the hydrolysis reaction of tetramethyl orthosilicate. Chem. Mater. **1990**, *2*, 372–376.
8. Osseo-Asare, K.; Arriagada, F.J. Preparation of SiO_2 nanoparticles in a nonionic reverse micellar system. Colloids Surf. **1990**, *50*, 321–339.
9. Wang, W.; Gu, B.; Liang, L.Y.; Hamilton, W. Fabrication of near infrared photonic crystals using highly-monodispersed submicrometer SiO_2-spheres. J. Phys. Chem. B **2003**, *107*, 12113–12117.

10. John, V.T.; Simmons, B.; McPherson, G.L.; Bose, A. Recent developments in materials synthesis in surfactant systems. Curr. Opin. Colloid Interf. Sci. **2002**, *7*, 288–295.
11. Antonietti, M. Surfactants for novel templating applications. Curr. Opin. Colloid Interf. Sci. **2001**, *6*, 244–248.
12. O'Sullivan, E.C.; Ward, A.J.I. Obvious and non-obvious influences of surfactants on the formation of nanosized particles. Langmuir **1994**, *10*, 2985–2992.
13. Iler, R.K. The chemistry of the silica. In *Polymerization of Silica*; John-Wiley & Sons: New York, 1979; Chap. 3.
14. Wang, W.; Gu, B.; Liang, L.; Hamilton, W. Fabrication of two- and three-dimensional silica nanocolloidal particle arrays. J. Phys. Chem. B **2003**, *107*, 3400–3404.
15. Lianos, P.; Zana, R. Fluorescence probe studies of the effect of concentration on the state of aggregation of surfactants in aqueous-solution. J. Colloid Interf. Sci. **1981**, *84*, 100–107.
16. Anderson, M.T.; Martin, J.E.; Odinek, J.G.; Newcomer, P.P. Effect of methanol concentration on CTAB micellization and on the formation of surfactant-templated silica (STS). Chem. Mater. **1998**, *10*, 1490–1500.
17. Atkin, R.; Craig, V.S.J.; Biggs, J. Adsorption kinetics and structural arrangements of cationic surfactants on silica surfaces. Langmuir **2000**, *16*, 9374–9380.
18. Kung, K-H.S.; Hayes, K.F. Fourier transform infrared spectroscopic study of the adsorption of cetyltrimethylammonium bromide and cetylpyridinium chloride on silica. Langmuir **1993**, *9*, 263–267.
19. Neivandt, D.J.; Gee, M.L.; Hair, M.L.; Tripp, C.P. Polarized infrared attenuated total reflection for the in situ determination of the orientation of surfactant adsorbed at the solid/solution interface. J. Phys. Chem. B **1998**, *102*, 5107–5114.
20. Snyder, R.G.; Scherer, J.R.; Gaber, B.P. Effects of chain packing and chain mobility on the Raman-spectra of biomembranes. Biochim. Biophys. Acta **1980**, *601*, 47–53.
21. Snyder, R.G. On Raman evidence for conformational order in liquid normal-alkanes. J. Chem. Phys. **1982**, *76*, 3342–3343.
22. Wong, P.T.T.; Mantsch, H.H. Temperature-induced phase-transition and structural-changes in micellar solutions of sodium oleate observed by Raman-scattering. J. Phys. Chem. **1983**, *87*, 2436–2443.
23. Kartha, V.B.; Leitch, L.C.; Mantsch, H.H. Infrared and Raman-spectra of alkali palmityl sulfates. Can. J. Chem. **1984**, *62*, 128–132.
24. Wang, W.; Li, L.; Xi, S. A Fourier transform infrared study of the coagel to micelle transition of cetyltrimethylammonium bromide. J. Colloid Interf. Sci. **1993**, *155*, 369–373.
25. Koglin, E.; Tarazona, A.; Kreisig, S.; Schwuger, M.J. In-situ investigations of coadsorbed cationic surfactants on charged surfaces: a SERS microprobe study. Colloids Surf. A **1997**, *123–124*, 523–542.
26. Okabayashi, H.; Okuyama, M.; Kitagawa, T.; Miyazawa, T. Raman-spectra and molecular-conformations of surfactants in aqueous-solution and crystalline states. Bull. Chem. Soc. Jpn. **1974**, *47*, 1075–1077.
27. Thompson, W.K. Vibrational-spectra of sodium dodecylsulfate 1-8 hydrate (alpha-phase). Spectrochim. Acta A **1974**, *30*, 117–124.
28. Picquart, M. Vibrational model behavior of SDS aqueous solutions studied by Raman scattering. J. Phys. Chem. **1986**, *90*, 243–250.
29. Sperline, R.P. Infrared spectroscopic study of the crystalline phases of sodium dodecyl sulfate. Langmuir **1997**, *13*, 3715–3726.
30. Koyama, Y.; Ikeda, K.-I. Raman-spectra and conformations of the cis-unsaturated fatty-acid chains. Chem. Phys. Lipids **1980**, *26*, 149–172.
31. Kobayashi, M.; Kaneko, F.; Sato, K.; Suzuki, M. Vibrational spectroscopic study on polymorphism and order-disorder phase transition in oleic acid. J. Phys. Chem. **1986**, *90*, 6371–6378.
32. Wang, W.; Efrima, S.; Regev, O. Directing oleate stabilized nanosized silver colloids into organic phases. Langmuir **1998**, *14*, 602–610.
33. Wang, W.; Chen, X.; Efrima, S. Silver nanoparticles capped by long-chain unsaturated carboxylates. J. Phys. Chem. B **1999**, *103*, 7238–7246.

Received December 10, 2003
Accepted February 25, 2004